

# Phase transformation and mechanical properties of B<sub>2</sub>O<sub>3</sub>-doped cordierite derived from complex-alkoxide

M. OKUYAMA\*, T. FUKUI†, C. SAKURAI‡  
*Colloid Research Institute Kitakyushu 805 Japan*

Cordierite gel powders doped with up to 3 mol% B<sub>2</sub>O<sub>3</sub> were prepared by the hydrolysis of an alkoxide complex. The effects of B<sub>2</sub>O<sub>3</sub>-doping on phase transformation were investigated for the purpose of preventing micro-cracking due to  $\mu$ - $\alpha$  cordierite transformation. B<sub>2</sub>O<sub>3</sub>-doping retarded the crystallization from amorphous to  $\mu$ -cordierite, and accelerated the crystallization of  $\alpha$ -cordierite. High doping concentrations (e.g. 1.5 mol%) appeared to promote the direct formation of  $\alpha$ -cordierite from the amorphous state. The development of microcracks due to the  $\mu$ - $\alpha$  cordierite transformation was prevented by the modified crystallization characteristics. The flexural strengths of the sintered bodies reached 190 MPa. B<sub>2</sub>O<sub>3</sub>-doping also lowered the temperatures of densification and crystallization of  $\alpha$ -cordierite to 850 and 950 °C, respectively. At the sintering temperatures of 1100 °C or above, however, glassy phase oozed out on to the surfaces and internal pores were formed in the sintered bodies, resulting in decreased flexural strength.

## 1. Introduction

Cordierite (2MgO–2Al<sub>2</sub>O<sub>3</sub>–5SiO<sub>2</sub>) or cordierite-based glass-ceramics are attractive materials for microelectronic packaging, because of their low dielectric constants, low thermal expansion coefficients, and other features [1–3]. Low-temperature processing (e.g. < 1000 °C) is also desired for the application of multilayered substrates, which can be co-fired with good electrical conductors such as gold, silver and copper [1–3]. The alkoxide method offers potential for remarkable reductions in sintering and crystallization temperatures [4], motivating many researchers to synthesize cordierite gels or gel powders from metal alkoxides [5–11]. We studied the optimum synthesis [12] and hydrolysis [13] conditions of an alkoxide-complex precursor of cordierite to improve the morphology and chemical homogeneity of the powder, and obtained a chemically homogeneous, unagglomerated gel powder of about 0.2  $\mu$ m.

When preparing  $\alpha$ -cordierite ceramics from amorphous materials (e.g. glasses or gels), a major issue exists: that is, the development of microcracks due to  $\mu$ - $\alpha$  cordierite transformation.  $\alpha$ -cordierite phase always appears via  $\mu$ -cordierite phase. The  $\mu$ - $\alpha$  cordierite transformation causes a sudden volume expansion, and high stresses are formed which lead to cracking [14, 15]. Suzuki *et al.* [16] studied the sintering of an alkoxide-derived cordierite gel, and found that the micro-cracks were healed by increased sintering temperature or prolonged heating, and

obtained the strength of  $\alpha$ -cordierite of 100 MPa. To overcome the microcracking, however, modification of the whole crystallization characteristics (i.e.  $\mu$ - $\alpha$  phase transformation) may be essential.

In our previous study [17], one answer was found with epitaxial seeding, which promotes a direct formation of  $\alpha$ -cordierite from the amorphous state, leading to the successful prevention of the microcracking. Thus a high maximum flexural strength of 190 MPa was obtained. However, the strengths were widespread in the range 100–190 MPa, and appeared to be sensitive to the seeding process. For example, agglomerates of seed particles could cause defects in the sintered bodies, leading to poor strengths. For a seeding method, the process has to be strictly controlled.

Another answer may be doping with a nucleation agent. In conventional glass-ceramics processing, a nucleation agent such as TiO<sub>2</sub>, ZrO<sub>2</sub>, or P<sub>2</sub>O<sub>5</sub> is usually added to the original glass to control the crystallization behaviour and achieve fine-grained crystallization. The addition of the nucleation agent may also be effective to modify the phase transformation of cordierite gel powder. There are, however, few studies on cordierite gel powder doped with a nucleation agent, and no successful report about the prevention of micro-cracking. In our previous study [18], ZrO<sub>2</sub> was added to a gel powder of stoichiometric cordierite composition. However, the addition increased the crystallization temperature of  $\alpha$ -cordierite and microcracks also developed.

\* Present address: R&D Center, NGK Spark Plug Co. Ltd, Iwasaki, Komaki, Aichi, 485 Japan.

† Present address: Kurosaki Refractories Co. Ltd, Kitakyushu, 806 Japan.

‡ Present address: Nippon Steel Co. Kawasaki, 100-71 Japan.

As a result of the exploration of several dopants,  $B_2O_3$  was found to be the only effective dopant which controls the crystallization of cordierite gel powder. In the present work, the effects of  $B_2O_3$ -doping in a homogeneous cordierite gel powder on the crystallization (i.e.  $\mu$ - $\alpha$  transformation) and microcrack formation were studied.

## 2. Experimental procedure

### 2.1. Powder preparation

$Si(OC_2H_5)_4$  dissolved in ethanol was partially pre-hydrolysed with HCl-catalysed water for 40 min in an ice-bath at a  $H_2O/HCl/Si(OC_2H_5)_4$ /ethanol molar ratio of 1.2/0.01/1/6.9.  $Al(OC_4H_9)_3$  was poured into dry ethanol in a nitrogen glove box at an  $Al(OC_4H_9)_3$ /ethanol molar ratio of 1/10.7, resulting in immediate precipitation of white solids. The two alkoxide component liquids thus obtained were mixed and refluxed until an optically clear solution was obtained. Magnesium metal flakes were added to the refluxed solution, followed by additional refluxing for 12 h. Magnesium metal was completely consumed, and a transparent solution of an alkoxide-complex precursor of cordierite was obtained. A desired amount of  $B(OC_2H_5)_3$  was added to the alkoxide-complex solution in the nitrogen glove box, and the solution was refluxed for 2 h. The solution was diluted with ethanol to an alkoxide concentration of about 13.2 wt %, and hydrolysed with 25 times the stoichiometric amount of 1 N  $NH_4OH$  water required for complete hydrolysis. A precipitated powder was filtered and dried at 150 °C in air without washing.

### 2.2. Sintering and characterization

The morphology of the powders was observed using a scanning electron microscope (SEM).  $B_2O_3$  contents in the powders were determined by inductively coupled plasma spectrometry (ICP) analysis. The crystallization behaviour was studied using a differential thermal analyser (DTA).

After calcination at 500 °C for 1 h, the powder was mixed with 3 wt % organic binder in ethanol by using a small alumina ball mill, and uniaxially pressed at 50 MPa, followed by hydrostatic pressing at 150 MPa. The resultant particle compacts of  $15 \times 35 \times 4$  mm<sup>3</sup> were calcined at 250 °C and fired at different temperatures for 1 h at a heating rate of 1 °C min<sup>-1</sup>. Densities for the sintered bodies were measured by the

Archimedes method. Crystalline phases formed in the sintered bodies were identified using an X-ray diffractometer (XRD). The microstructure was observed using a scanning electron microscope (SEM). The fracture strength was measured by the three-point bending method.

## 3. Results and discussion

### 3.1. Powder characterization

$B_2O_3$ -doping in cordierite gel powders was attempted with different concentrations of  $B_2O_3$  (0, 0.5, 1, 2.5, and 5 mol %). In our previous study [13], the yield of cordierite powder was almost 100% under the hydrolysis conditions used in this study. When preparing a borosilicate powder from metal alkoxides, however, a concern is the yield of  $B_2O_3$  [19]; boron species may remain in the supernatant liquid, probably because of the high solubility in alcohol-water systems. Thus the amounts of  $B_2O_3$  in the powders obtained were determined by ICP analysis (Table I). The  $B_2O_3$  contents analysed were considerably lower than those of the corresponding preparation compositions. Under the experimental conditions used in this study, the yields were in the range of 54%–59%. These powders were designated B-0, B-0.3, B-0.6, B-1.5, and B-3.0, respectively, in which the numerals roughly indicate the  $B_2O_3$  contents (mol %) determined by ICP.

Fig. 1 shows the typical morphology of  $B_2O_3$ -doped powder (B-1.5).  $B_2O_3$ -doped cordierite powder consisted of discrete particles with particle sizes ranging from 0.1–0.3  $\mu$ m, although they were slightly aggregated. The specific surface area measured by the BET method was about 150 m<sup>2</sup> g<sup>-1</sup>, suggesting these particles were porous. The morphology was similar to that of undoped gel powder (B-0), and differences caused by  $B_2O_3$ -doping were not observed.

### 3.2. Crystallization

Fig. 2 shows the DTA curves of undoped and  $B_2O_3$ -doped cordierite gel powders at a heating rate of 10 °C min<sup>-1</sup>. The undoped cordierite gel powder (B-0) showed two separate exothermic peaks at 932 and 1040 °C. These two peaks were identified as the crystallization exotherms of amorphous to  $\mu$ -cordierite and the transformation of  $\mu$ - $\alpha$  cordierite, respectively, by XRD. As the amount of  $B_2O_3$  increased, the exothermic peak at 932 °C due to the crystallization of  $\mu$ -phase shifted to higher temperatures and the peak

TABLE I  $B_2O_3$  contents in cordierite gel powders

Designation	Preparation composition <sup>a</sup> (mol %)				ICP analysis, $B_2O_3$ (mol %)	Yield <sup>b</sup> $B_2O_3$ (%)
	$B_2O_3$	MgO	$Al_2O_3$	$SiO_2$		
B-0	–	22.2	22.2	55.6	–	–
B-0.3	0.5	22.1	22.1	55.3	0.27 ± 0.01	54.3
B-0.6	1.0	22.0	22.0	55.0	0.57 ± 0.01	57.4
B-1.5	2.5	21.7	21.7	54.2	1.46 ± 0.05	58.4
B-3.0	5.0	21.1	21.1	52.8	2.93 ± 0.03	58.7

<sup>a</sup> MgO/ $Al_2O_3$ / $SiO_2$  = 2/2/5 (mole ratio).

<sup>b</sup> Yield =  $B_2O_3(ICP)/B_2O_3(preparation)$ .

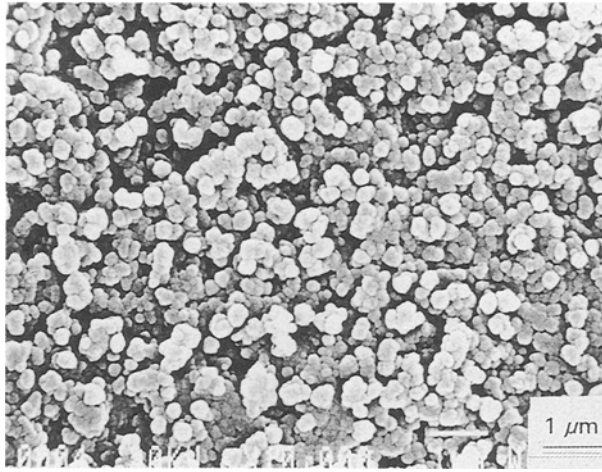


Figure 1 Scanning electron micrograph of  $B_2O_3$ -doped cordierite gel powder (B-1.5).

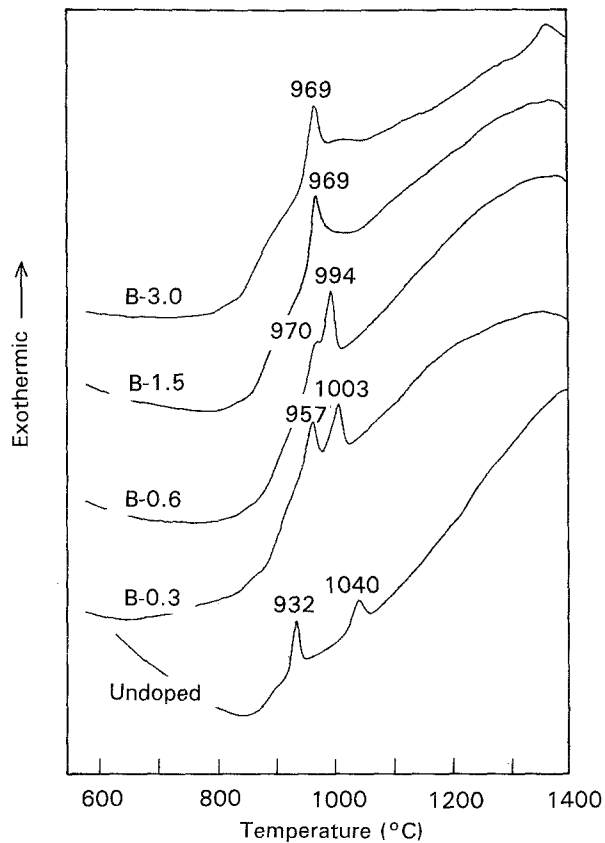


Figure 2 DTA curves of undoped and  $B_2O_3$ -doped cordierite gel powders. Numerals indicate the temperatures of the maxima of the DTA peaks.

height decreased. Concurrently, the other exothermic peak at  $1040^\circ\text{C}$  due to the transformation to the  $\alpha$ -phase shifted to lower temperatures. For high concentrations of doping (B-1.5 and B-3.0), only a single peak was observed at  $969^\circ\text{C}$ .

Figs 3 and 4 show the XRD patterns of the sintered bodies obtained from undoped (B-0) and  $B_2O_3$ -doped (B-1.5) powders, respectively. The B-0 remained amorphous up to  $850^\circ\text{C}$ , crystallized to  $\mu$ -cordierite at  $900^\circ\text{C}$  for 1 h, and transformed into single phase  $\alpha$ -cordierite by firing at  $1050^\circ\text{C}$  for 1 h. B-1.5 also remained amorphous at  $850^\circ\text{C}$  for 1 h. When fired at

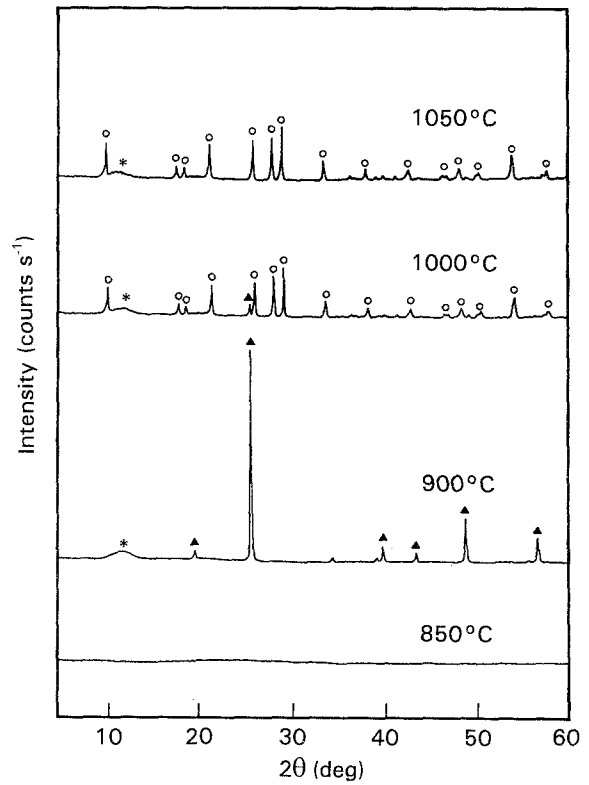


Figure 3 X-ray diffraction patterns of undoped samples (B-0) fired at different temperatures for 1 h: (○)  $\alpha$ -cordierite, (▲)  $\mu$ -cordierite, (\*) cellophane tape used to fix sample to XRD holder.

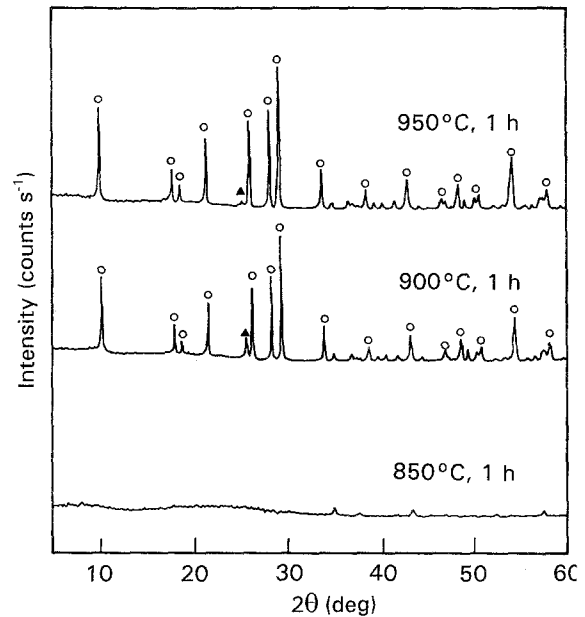


Figure 4 X-ray diffraction patterns of  $B_2O_3$ -doped samples (B-1.5) fired at different temperatures for 1 h. (○)  $\alpha$ -cordierite, (▲)  $\mu$ -cordierite.

$900^\circ\text{C}$  for 1 h, however, the dominant phase formed in B-1.5 sample was  $\alpha$ -cordierite and only a trace of  $\mu$ -cordierite was observed. On firing at  $950^\circ\text{C}$  for 1 h, B-1.5 had crystallized to almost single phase  $\alpha$ -cordierite. Thus the doping of 1.5 mol %  $B_2O_3$  lowered the crystallization temperature of  $\alpha$ -cordierite from  $1050^\circ\text{C}$  to  $950^\circ\text{C}$ . In all cases, no other phases such as spinel or  $\text{SiO}_2$ -rich  $\beta$ -quartz solid solution, were detected by XRD.

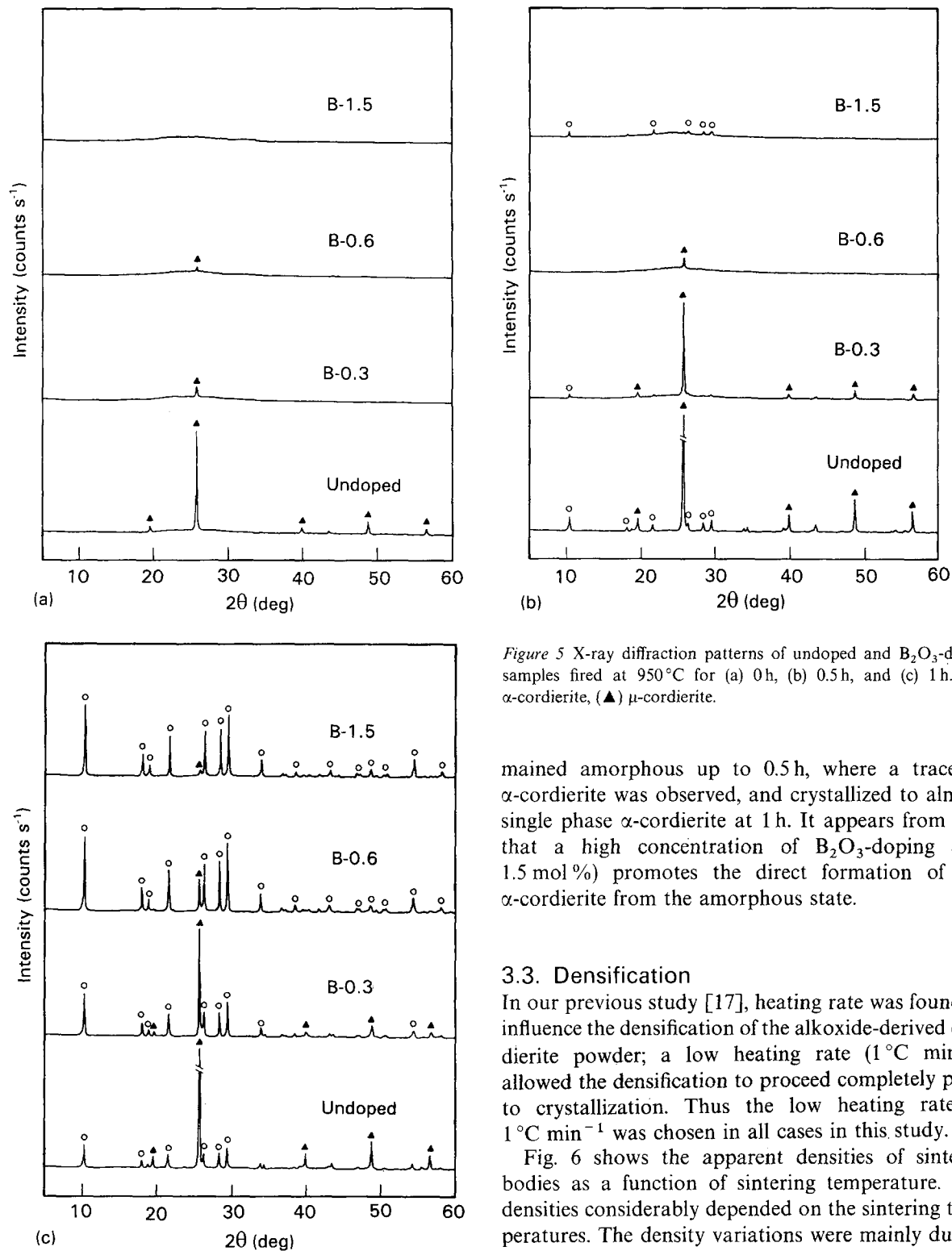


Figure 5 X-ray diffraction patterns of undoped and  $B_2O_3$ -doped samples fired at  $950^\circ C$  for (a) 0h, (b) 0.5h, and (c) 1h. (○)  $\alpha$ -cordierite, (▲)  $\mu$ -cordierite.

Fig. 5 shows the change in XRD patterns for undoped and doped samples fired at  $950^\circ C$  for different holding times. With increasing  $B_2O_3$  content, the crystallization of  $\mu$ -cordierite was retarded, while that of  $\alpha$ -cordierite was accelerated. This trend is consistent with the DTA result. It is noteworthy that  $B_2O_3$ -doping showed opposing effects (i.e. negative and positive) on the crystallization of  $\mu$ - and  $\alpha$ -cordierite. The crystallization behaviour of B-1.5 was considerably different from that of undoped powder (B-0). The crystallization of B-0 was consistent with the previous reports [5–11];  $\alpha$ -cordierite phase appeared via  $\mu$ -cordierite phase. However, B-1.5

mained amorphous up to 0.5h, where a trace of  $\alpha$ -cordierite was observed, and crystallized to almost single phase  $\alpha$ -cordierite at 1h. It appears from this that a high concentration of  $B_2O_3$ -doping (e.g. 1.5 mol %) promotes the direct formation of the  $\alpha$ -cordierite from the amorphous state.

### 3.3. Densification

In our previous study [17], heating rate was found to influence the densification of the alkoxide-derived cordierite powder; a low heating rate ( $1^\circ C \text{ min}^{-1}$ ) allowed the densification to proceed completely prior to crystallization. Thus the low heating rate of  $1^\circ C \text{ min}^{-1}$  was chosen in all cases in this study.

Fig. 6 shows the apparent densities of sintered bodies as a function of sintering temperature. The densities considerably depended on the sintering temperatures. The density variations were mainly due to the differences in crystalline phases formed in the sintered bodies. For undoped powder, high densities of the samples fired at  $900$  or  $950^\circ C$  were due to the higher density  $\mu$ -cordierite phase. At the sintering temperatures of  $1050^\circ C$  or above, the undoped samples transformed to  $\alpha$ -cordierite and the densities were close to the theoretical value of  $\alpha$ -cordierite ( $2.512 \text{ g cm}^{-3}$ ).

$B_2O_3$ -doped powders (i.e. B-1.5 or B-3.0) appeared to be fully densified on firing at  $850^\circ C$  for 1h. The densification temperatures for these samples were  $50^\circ C$  lower than that of the undoped powder, which is consistent with well-known effect of  $B_2O_3$ ;  $B_2O_3$  additions to silicate gels reduce the temperatures required for viscous sintering [19]. B-1.5 and B-3.0 samples

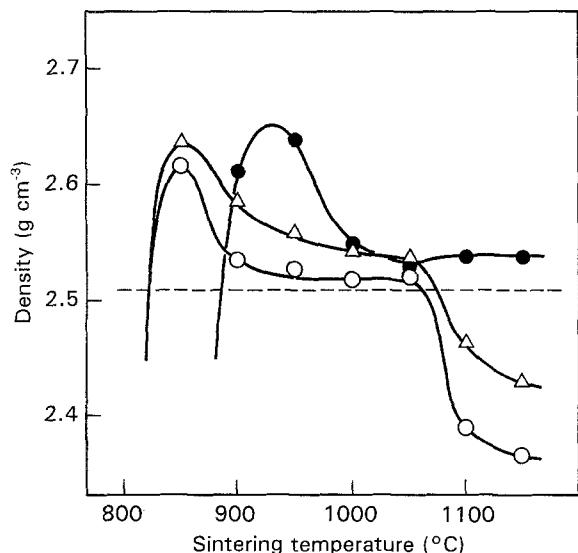


Figure 6 Apparent densities of (●) undoped and (Δ) B-1.5 and (○) B-3.0 samples as a function of sintering temperature. (—) Theoretical density of  $\alpha$ -cordierite.

fired at 900°C were amorphous and showed high densities, compared with that of  $\alpha$ -cordierite. The density decreased with increasing sintering temperature, owing to the crystallization to the lower density  $\alpha$ -cordierite phase. When fired at 950–1050°C, the density almost reached the theoretical value. These sintered bodies had dense microstructure, as shown in Fig. 7a, where only very fine pores ( $< 0.1 \mu\text{m}$ ) are observed.

At sintering temperatures of 1100°C or above, however, the density considerably decreased to the values lower than that of  $\alpha$ -cordierite. For these samples, a glassy layer on the surfaces was observed with the naked eyes. The scanning electron micrograph of the fracture surface (Fig. 7b) shows many large pores ( $> 1 \mu\text{m}$ ), which lead to the low densities. On firing at temperatures exceeding 1100°C,  $\text{B}_2\text{O}_3$  component could be excluded to the grain boundary, owing to the complete crystallization of  $\alpha$ -cordierite, and the  $\text{B}_2\text{O}_3$ -rich glassy phase with low viscosity could ooze out on to the surface, leaving large internal pores. Thus the optimum sintering temperatures for B-1.5 and B-3.0 were found to lie in the range 950–1050°C.

### 3.4. Mechanical property

Fig. 8 shows the flexural strengths of undoped and doped samples fired at different temperatures for 1 h. The undoped samples fired at 900°C, consisting of  $\mu$ -cordierite, showed the average fracture strength of 160 MPa. However, once the undoped samples were fired at temperatures exceeding 900°C, the strengths rapidly decreased to about 30 MPa, owing to  $\mu$ - $\alpha$  transformation. Microcracking had occurred in these samples exclusively, because the  $\mu$ - $\alpha$  transformation caused a sudden volume expansion and formed high stress [14, 15].

For powders doped with  $\text{B}_2\text{O}_3$  (B-1.5 and B-3.0), no microcracks were observed in the sintered samples, although they had crystallized to  $\alpha$ -cordierite. B-1.5 or B-3.0 samples fired at 950–1050°C showed high flex-

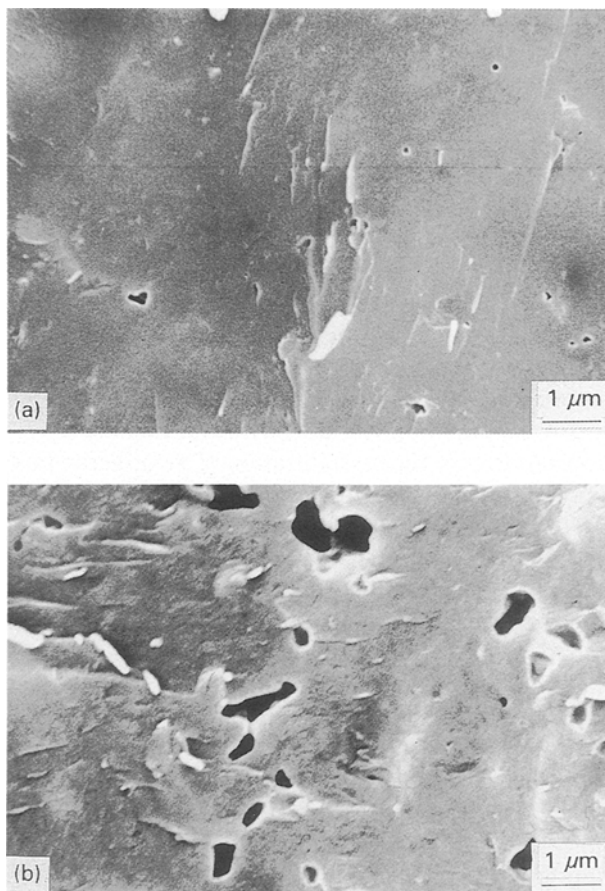


Figure 7 Scanning electron micrographs of fracture surfaces of  $\text{B}_2\text{O}_3$ -doped samples (B-1.5) fired at (a) 1000°C and (b) 1150°C for 1 h.

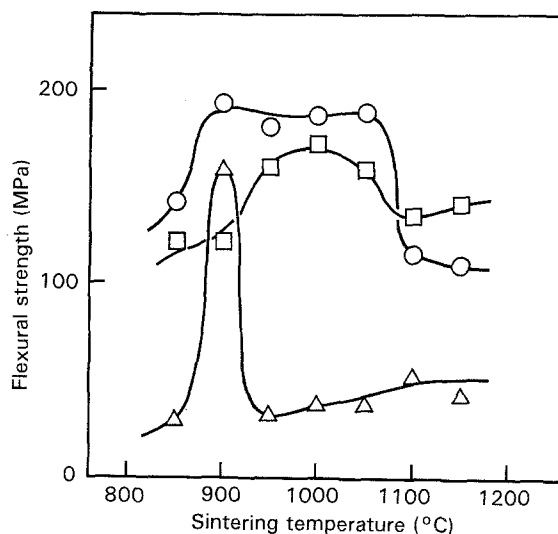


Figure 8 Flexural strengths of (Δ) undoped and (□) B-1.5 and (○) B-3.0 samples as a function of sintering temperature.

ural strengths ranging from 160–190 MPa. The high strength was probably due to the crack-free dense microstructure with only small defects (see Fig. 7a). When fired at 1100°C or above, however, the strength decreased. This was most likely due to the poor microstructure with large defects of  $> 1 \mu\text{m}$  (see Fig. 7b).

In this study, the doping of  $\text{B}_2\text{O}_3$  has been demonstrated as leading to the successful prevention of microcracking in  $\alpha$ -cordierite ceramics. This could be

attributed to the modification of crystallization characteristics by the  $B_2O_3$ -doping. A major difference was observed in the crystallization characteristics between undoped and  $B_2O_3$ -doped powders. For the undoped powder,  $\alpha$ -cordierite appeared from the crystalline matrix consisting of  $\mu$ -cordierite. Because the crystalline matrix does not allow stress relief, the sudden increase in volume due to the  $\mu$ - $\alpha$  transformation leads to the development of severe microcracks. For  $B_2O_3$ -doped powders, the doping appeared to stabilize the amorphous state, and promoted the direct formation of the  $\alpha$ -cordierite from the amorphous state. Thus the volume change due to the  $\mu$ - $\alpha$  transformation could be avoided. For the  $B_2O_3$ -doped powders, the crystallization of  $\alpha$ -cordierite possibly causes another volume change, because the density of the amorphous state was higher than that of  $\alpha$ -cordierite (see Fig. 6). However, this volume change occurs in the amorphous matrix, not from the crystalline matrix as for undoped powder. The amorphous matrix could be very viscous. Thus plastic flow of the matrix could be sufficient to relax the stress, and does not cause the high stresses leading to cracking.

Among the dopants explored in our laboratory (including  $ZrO_2$  [18],  $TiO_2$ , and  $P_2O_5$ ),  $B_2O_3$  was the only effective dopant which modified the crystallization of cordierite gel powder. The effect of  $B_2O_3$ -doping was specific, and considerably different from that of the other dopants. It should be investigated further why and how only  $B_2O_3$  promotes the direct formation of  $\alpha$ -cordierite.

#### 4. Conclusion

$B_2O_3$  was found to be the specific dopant which promoted the direct formation of  $\alpha$ -cordierite from the amorphous state. The  $B_2O_3$ -doping in a cordierite gel powder showed opposing effects (i.e. negative and positive) on the crystallization of  $\mu$ - and  $\alpha$ -cordierite, respectively, and promoted the direct formation of the  $\alpha$ -phase for high concentrations of doping (e.g. 1.5 mol %). The crystallization characteristics modified by  $B_2O_3$ -doping led to the successful prevention of the microcracking due to the  $\mu$ - $\alpha$  cordierite transformation. The sintered bodies showed a dense microstructure, and the flexural strength reached 190 MPa.

#### Acknowledgements

The authors thank Professor M. Yamane for invaluable discussions, and K. Higashi for technical assistance.

#### References

1. A. H. KUMAR, P. W. McMILLAN and R. R. TURMMALA, US Pat. 4301324, November 1981.
2. R. R. TURMMALA, *J. Am. Ceram. Soc.* **74** (1991) 895.
3. K. KONDO, M. OKUYAMA and Y. SHIBATA, in "Multi-layer Ceramic Devices", edited by J. B. Blum, and W. R. Cannon (American Ceramic Society, Columbus, OH, 1986) p. 77.
4. E. BARRINGER, N. JUBB, B. FEGLEY, R. L. POBER and H. K. BOWEN, in "Ultrastructure Processing of Ceramics, Glasses, and Composites", edited by L. L. Hench and D. R. Ulrich (Wiley, New York, 1984) p. 315.
5. J. C. BERNIER, J. L. REHSPRINGER, S. VILMINOT and P. POIX, in "Better Ceramics Through Chemistry II", edited by C. J. Brinker, D. E. Clark and D. R. Ulrich (Materials Research Society, Pittsburgh, PA, 1986) p. 129.
6. C. GENSSE and U. CHOWDHRY, *ibid.* p. 693.
7. H. SUZUKI, K. OTA and H. SAITO, *Yogyo-Kyokai-Shi* **95** (1987) 163.
8. A. B. HARDY, G. GOWDA, T. J. McMAHON, R. E. RIMAN, W. E. RHINE and H. K. BOWEN, in "Ultrastructure Processing of Advanced Ceramics", edited by J. D. Mackenzie and D. R. Ulrich (Wiley, New York, 1988) p. 407.
9. T. J. McMAHON, MS thesis, Department of Materials Science and Engineering, Massachusetts Institute of Technology, Cambridge, MA (1987).
10. F. BABONNEAU, L. COURY and J. LIVAGE, *J. Non-Cryst. Solids* **121** (1990) 153.
11. U. SELVARAJ, S. KOMARNENI and R. ROY, *J. Am. Ceram. Soc.* **73** (1990) 3663.
12. M. OKUYAMA, T. FUKUI and C. SAKURAI, *ibid.* **75** (1992) 153.
13. *Idem*, *J. Non-Cryst. Solids*, **144** (1992) 298.
14. B. H. MUSSLER and M. W. SHAFER, *Am. Ceram. Soc. Bull.* **64** (1985) 1459.
15. T. I. BARRY, J. M. COX and R. MORRELL, *J. Mater. Sci.* **13** (1978) 594.
16. H. SUZUKI, K. OTA and H. SAITO, *ibid.* **23** (1988) 1534.
17. M. OKUYAMA, T. FUKUI and C. SAKURAI, *J. Mater. Res.* **7** (1992) 2281.
18. M. OKUYAMA, T. FUKUI and C. SAKURAI, in "Ceramic Powder Science IV", edited by S. Hirano, G. L. Messing, and H. Hausner (American Ceramic Society, Columbus, OH, 1992) p. 675.
19. N. J. JUBB and H. K. BOWEN, *J. Mater. Sci.* **22** (1987) 1963.

Received 18 May 1992

and accepted 11 January 1993